Weber, K., & Konigsberg, W. (1975) in *RNA Phages* (Zinder, N., Ed.) pp 51–84, Cold Spring Harbor Laboratory, Cold Spring Harbor, NY.
Winter, R. B., & von Hippel, P. H. (1981) *Biochemistry 20*, 6948–6960.
Yarus, M., & Berg, P. (1967) *J. Mol. Biol. 28*, 479–490.
Yates, J. L., Arfsten, A. E., & Nomura, M. (1980) *Proc. Natl. Acad. Sci. U.S.A. 77*, 1837–1841.
Zagorska, L., Chroboczek, J., & Zagorski, W. (1975) *J. Virol. 15*, 509–514.

Kinetic and Thermodynamic Characterization of the R17 Coat Protein–Ribonucleic Acid Interaction†

Jannette Carey and Olke C. Uhlenbeck*

ABSTRACT: A filter retention assay is used to examine the kinetic and equilibrium properties of the interaction between phage R17 coat protein and its 21-nucleotide RNA binding site. The kinetics of the reaction are consistent with the equilibrium association constant and indicate a diffusion-controlled reaction. The temperature dependence of K_a gives $\Delta H = -19$ kcal/mol. This large favorable ΔH is partially offset by a $\Delta S = -30$ cal mol^{-1} deg^{-1} to give a $\Delta G = -11$ kcal/mol at 2 °C in 0.19 M salt. The binding reaction has a pH optimum centered around pH 8.5, but pH has no effect on ΔH. While the interaction is insensitive to the type of monovalent cation, the affinity decreases with the lyotropic series among monovalent anions. The ionic strength dependence of K_a reveals that ionic contacts contribute to the interaction. Most of the binding free energy, however, is a result of nonelectrostatic interactions.

The binding of regulatory proteins to nucleic acids is fundamental to the control of gene expression. It is of interest to understand the nature and relative importance of the elements which confer specificity on such interactions. One useful approach has been to reproduce the binding reaction with purified components, determine the association constant, and observe the effect of changing solution conditions on the association constant. When this approach has been applied to several DNA–protein binding systems, inferences have been made about the mechanism and molecular basis for these interactions (de Haseth et al., 1977; Strauss et al., 1980; Barkley et al., 1981; Winter et al., 1981). The previous paper (Carey et al., 1983) established that the interaction of R17 coat protein with a synthetic 21-nucleotide binding site is an excellent example of a simple, sequence-specific RNA–protein binding system. In the present paper, the association constant of the coat protein–21-mer[1] interaction is determined under a variety of solution conditions. The kinetics of the binding reaction are also presented. The results are interpreted in terms of the types of contacts made between the protein and nucleic acid and of the relative contributions of the various types of contacts to the free energy of the interaction. The results are compared with those of similar experiments on DNA–protein interactions to highlight certain differences in binding properties that can be attributed to the structural differences between the two nucleic acid targets.

Materials and Methods

The synthesis of the internally ^{32}P-labeled 21-nucleotide binding fragment is described in Krug et al. (1982). The specific activity averaged 2000 Ci/mmol. The isolation of R17 coat protein and the details of the nitrocellulose filter retention assay are described in Carey et al. (1983). For the various buffers used in this work, the pH was adjusted at the temperature used in the incubation. Standard TMK buffer is 0.1 M Tris-HCl, pH 8.5 at 2 °C, 10 mM magnesium acetate, and 80 mM KCl.

Results

Kinetics. The dissociation rate of the coat protein–RNA complex was measured by forming complexes between ~10 pM ^{32}P-labeled 21-mer and several different protein concentrations (5–60 nM). Two different methods, both based on the filter retention assay, were used to follow the dissociation kinetics. In the first method, dissociation of complexes formed with labeled 21-mer was observed by adding 50 nM unlabeled intact R17 RNA. Since R17 RNA competes effectively with the 21-mer (Carey et al., 1983) and is added in 10-fold molar excess over coat protein, dissociated 21-mer must compete with the unlabeled RNA to rebind to the protein, resulting in reduction of the amount of labeled 21-mer in the complexes with time until a new equilibrium is established. An example of this first type of dissociation experiment is shown in Figure 1A. A control experiment in which unfractionated *Escherichia coli* tRNA is added at zero time shows no decrease in the amount of bound 21-mer with time. Since tRNA does not compete with the 21-mer, this result indicates that once the labeled 21-mer has dissociated it can rebind the protein during the period of the experiment. In the second method, dissociation was initiated by diluting the reaction 5- or 10-fold with buffer, and samples were withdrawn and filtered at intervals until the new equilibrium was reached. Since it was previously shown that complexes trapped on the filter do not dissociate any further, the filtration procedure will accurately determine

† From the Department of Biochemistry, University of Illinois, Urbana, Illinois 61801. *Received November 17, 1982.* This work was supported by a grant from the National Institutes of Health (GM 19059).

[1] Abbreviations: 21-mer, 21-nucleotide synthetic RNA fragment comprising residues −17 to +4 of the R17 RNA, where +1 is the first nucleotide of the replicase gene; Tris, 2-amino-2-(hydroxymethyl)-1,3-propanediol; Hepes, 4-(2-hydroxyethyl)-1-piperazineethanesulfonic acid; Mes, 2-(*N*-morpholino)ethanesulfonic acid; Ches, 2-(*N*-cyclohexylamino)ethanesulfonic acid; EDTA, ethylenediaminetetraacetic acid.

0006-2960/83/0422-2610$01.50/0

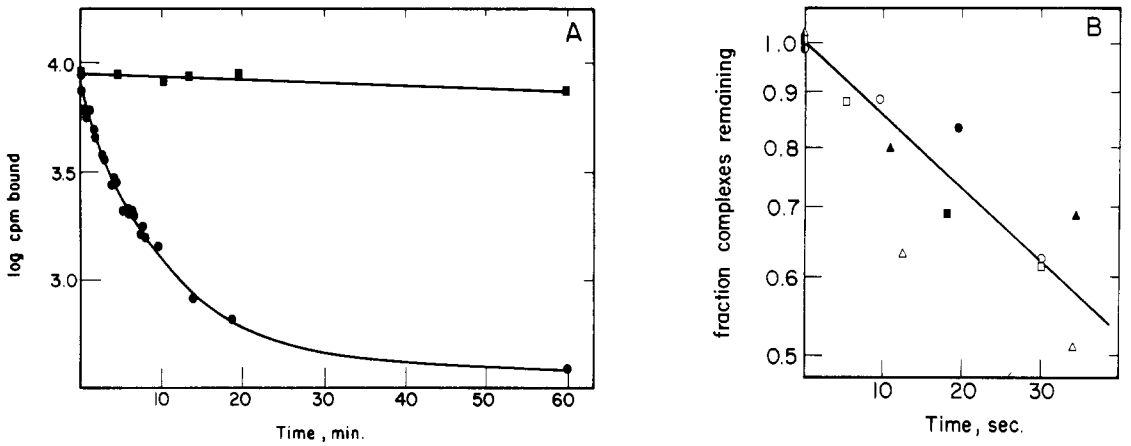

FIGURE 1: Dissociation kinetics of coat protein–21-mer complexes. (A) At zero time, either 50 nM R17 RNA (●) or 50 nM *E. coli* tRNA (■) was added to a complex of ~10 pM ^{32}P-labeled 21-mer and 5 nM coat protein in TMK at 2 °C. At the indicated times, 250-μL aliquots were filtered without dilution or washing. (B) Initial rate of dissociation in TMK. Open symbols, dissociation rate measured by the addition of a 10-fold molar excess of R17 RNA to complexes of ~10 pM ^{32}P-labeled 21-mer and 30 nM (○) or 5 nM (□) coat protein or ~10 pM ^{32}P-labeled 59-mer and 5 nM coat protein (△). Closed symbols, dissociation rate of complexes formed with 10 pM ^{32}P-labeled 21-mer measured by dilution from 10 to 2 nM (●), from 60 to 6 nM (■), or from 20 to 2 nM (▲) coat protein. The solid line is k_{off} = 0.012 s^{-1}.

the amount of complex remaining at each time. Figure 1B shows the early time points from experiments using several different protein concentrations and both methods for measuring the dissociation rate. The two methods give essentially identical results. As expected for a unimolecular decomposition, the initial rate is independent of the coat protein concentration. From the slope of Figure 1B, a value of k_{off} = 0.012 s^{-1} can be determined, corresponding to a half-life of 58 s for the complex. The 59-mer and 21-mer behave similarly.

In an attempt to determine the association rate constant between the RNA and coat protein, approximately 10 pM labeled 21-mer was mixed with several different coat protein concentrations (0.1–100 nM), and aliquots were withdrawn and filtered after very short intervals. Previous experiments demonstrated that little if any RNA binds to protein already bound to the filter, so the filtration process effectively stops the association in about 3 s. Figure 2A shows the result obtained with 7 nM protein. The amount of complex increases rapidly to half-maximum at 30 s, and a plateau is reached at about 200 s. When similar experiments were carried out at higher coat protein or RNA concentrations, complex formation was essentially complete at the earliest feasible time points (10 s), so adequate rate data could not be obtained. When protein concentrations less than 3 nM were used with ~10 pM RNA, the amount of complex formed was so small that the reproducibility of the data was very poor. RNA of higher specific activity could not easily be prepared, so lower RNA concentrations were not used. Reliable rate data were therefore obtained only at ~10 pM RNA and from 3 to 7 nM coat protein. The accessible range is thus too limited to obtain the data necessary to plot rate vs. coat protein concentration at several RNA concentrations, as would be required to determine the true association rate constant. An estimate of the association rate constant can be obtained, however, from the initial rate observed in Figure 2A by assuming that little dissociation occurs at very early times. The solid line in Figure 2B is the theoretical rate calculated from the integrated rate equation for a bimolecular reaction [e.g., see eq 7 of Riggs et al. (1970)] for the first four points in Figure 2A with k_{on} = 9.4 × 10^5 M^{-1} s^{-1}.

The estimate of the forward rate constant can be divided by the value of the dissociation rate constant to obtain a calculated association constant of 7.8 × 10^7 M^{-1}. This value

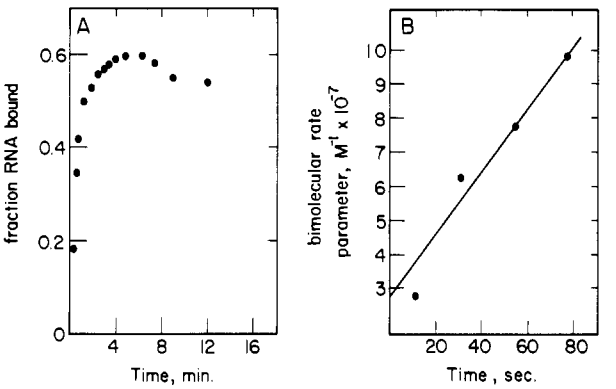

FIGURE 2: (A) Association kinetics of 7 nM coat protein and 10 pM ^{32}P-labeled 21-mer in TMK at 2 °C. At the indicated times, 450-μL aliquots were withdrawn and filtered. (B) Bimolecular rate parameter [defined in eq 7 of Riggs et al. (1970)] calculated for the first four points in (A) by assuming k_{off} = 0. The line is k_{on} = 9.4 × 10^5 M^{-1} s^{-1}.

is within a factor of 4 of the association constant of 3 × 10^8 M^{-1} obtained by Carey et al. (1983) under the same solution conditions, consistent with the notion that complex formation obeys a bimolecular equilibrium. The agreement between the two determinations of K_a may not be better due to the inaccuracies involved in estimating the forward rate constant.

pH Dependence of K_a. The pH optimum for the coat protein–RNA interaction was determined by measuring K_a at different values of pH. A series of buffers was prepared which contained 10 mM magnesium acetate, 80 mM KCl, and 100 mM buffer adjusted to the desired pH at 2 °C. Although Tris-HCl was used throughout the pH range, buffers with more appropriate p*K*s were tested as well. In each buffer, a complete protein excess binding curve was obtained by using the filter assay. Briefly, a constant, low concentration of labeled 21-mer in buffer was mixed with varying concentrations of coat protein. Each reaction was then filtered without dilution or subsequent washing. Half-maximal retention of labeled 21-mer on the filter occurs at a coat protein concentration equal to K_d for complex formation, and $K_a = K_d^{-1}$. Figure 3 shows that a plot of log K_a as a function of pH is bell shaped with an optimum near pH 8.5. The shape of the curve indicates that at least two types of titratable groups can influence the protein–RNA interaction. For optimal binding,

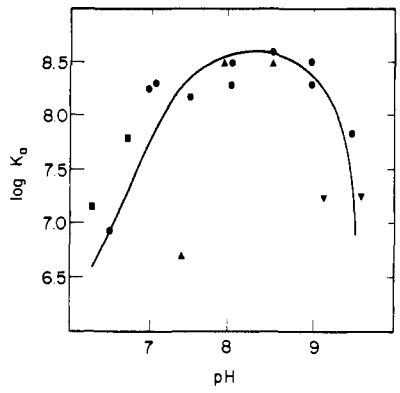

FIGURE 3: pH dependence of K_a. Protein excess binding curves were obtained at 2 °C in 10 mM magnesium acetate, 80 mM KCl, and 100 mM either of Tris-HCl (●), K-Mes (■), K-Hepes (▲), or of K-Ches (▼) adjusted to the indicated pH.

the pH must be high enough to deprotonate some group(s) with a pK near 7 but low enough so that some other group(s) with a pK near 9 remain protonated. The optimum pH is close to the pI of about 8 that is observed for denatured coat protein (J. Parker, personal communication). Since the 21-mer is not believed to have any titratable groups with pKs around 7, the ascending arm of Figure 3 must be due to the protonation of some group(s) on the coat protein. The absence of histidine from R17 coat protein (Weber, 1967) eliminates the most obvious possibility. The descending arm of Figure 3 cannot necessarily be attributed to deprotonation of an amino acid on the protein, since both guanine and uracil can deprotonate in this range as well.

de Haseth et al. (1977) estimated the number of groups being titrated from the slope of the linear part of the log K_a vs. pH profile. Although the data in Figure 3 are not accurate enough to determine the exact number of titratable groups responsible for the pH dependence of the coat protein–RNA interaction, the comparatively broad shape of the curve implies that only a few protons are involved at each of the two pKs.

Temperature Dependence of K_a. Protein excess binding curves were obtained as a function of temperature by using TMK buffer which had been adjusted to pH 8.5 at each temperature. Filtration was also carried out at the temperature indicated. The van't Hoff plot of these data is shown in Figure 4. The ΔH obtained from the line is −19 kcal/mol of complex. In the case of some DNA–protein interactions [e.g., see Strauss et al. (1980)], most of the observed enthalpy change is associated with protonation of groups on the protein. Since the data in Figure 3 indicated that protonation is important in the coat protein–RNA interaction, the effect of pH on ΔH was also examined. As seen in Figure 4, the van't Hoff plot is identical at pH 7, 8, and 9. Thus, ΔH is independent of pH in the range where titration effects are known to occur.

Effect of Solution Composition on K_a. The standard TMK buffer used in these experiments was identical with that of Gralla et al. (1974) except that the pH was increased from 7.5 to 8.5 to increase the K_a. A variety of other solution compositions were examined to determine their effect on the K_a of the coat protein–RNA interaction.

Figure 5 shows the effect on K_a of the identity of the cation (panel A) or the anion (panel B) of the 80 mM monovalent salt. In each case, 100 mM Tris-HCl, pH 8.5, and 10 mM magnesium acetate were present as well. Replacing potassium ion by sodium, lithium, or ammonium had no detectable effect upon K_a. The anion effects, on the other hand, are relatively large despite the fact that about 50 mM chloride ion and 10 mM acetate ion are also present in each reaction. The K_a

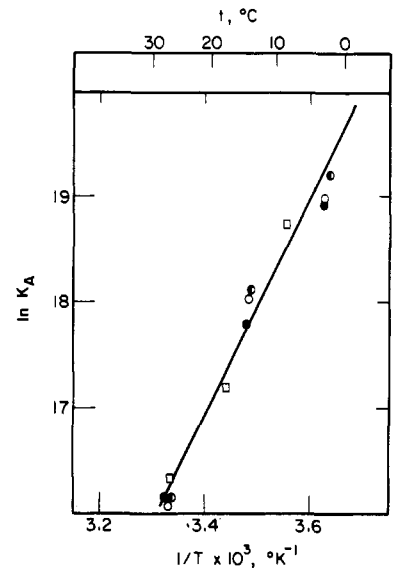

FIGURE 4: Temperature dependence of K_a. Protein excess binding curves were obtained in TMK adjusted to pH 7.0 (●), 8.0 (○), 8.5 (□), or 9.0 (◐) at the indicated temperatures. The line gives ΔH = −19 kcal/mol.

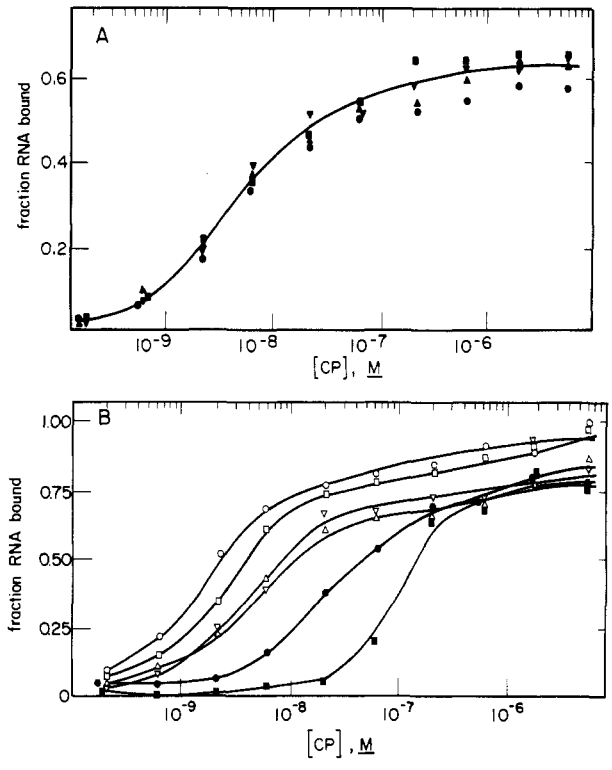

FIGURE 5: Effect of monovalent salt on K_a. Coat protein (CP) excess binding curves were obtained at 2 °C in 10 mM magnesium acetate, 100 mM Tris-HCl, pH 8.5, and 80 mM monovalent salt. (A) Various cations: LiCl (●); NaCl (■); KCl (▲); NH_4Cl (▼). (B) Various anions and K_d values determined from the binding curves: Na-CH_3COO (○, 2 nM); NaCl (□, 3 nM); NaBr (△, 4 nM); $NaNO_3$ (▽, 5 nM); NaSCN (●, 20 nM); NaI (■, 100 nM).

decreases about 50-fold in the order $CH_3CO_2^- > Cl^- > Br^- > NO_3^- > SCN^- > I^-$, which is consistent with the lyotropic series. At 80 mM anion concentration, the effect of lyotropic ions is probably due to a specific effect on the protein rather than to the general effect on solvent water structure seen at higher ion concentrations (von Hippel & Schleich, 1969).

The effect of divalent cation identity and concentration was also examined. Protein excess binding curves were obtained

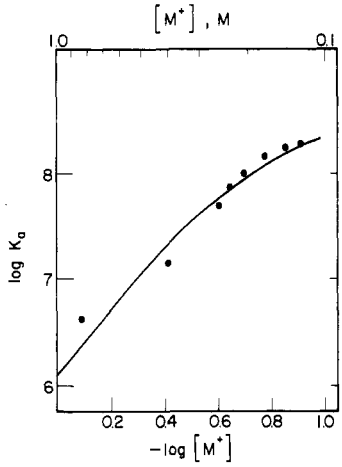

FIGURE 6: Ionic strength dependence of K_a. Protein excess binding curves were obtained in TMK buffer with KCl added to give the indicated total cation concentration, $[M^+]$. The solid line is calculated from the ion displacement model for $Z = 4.7$ and $\log K_{1M} = 6.25$ with the assumptions that the affinity of Mg^{2+} for the 21-mer is described by $\log K_{Mg} = 0.96 - 1.63 \log [M^+]$, $\psi = 0.85$, and that anion effects can be neglected.

with Cu^{2+}, Ca^{2+}, or Mg^{2+} concentrations ranging from 0 to 0.5 M; either the acetate or the chloride salt was used with identical results. TMK buffer lacking Mg^{2+} was made 0.5 mM in Na_2EDTA to achieve 0 M divalent cation. In many independent experiments, the absence of Mg^{2+} caused variable retention efficiency in the plateau region of the binding curve, precluding exact determination of K_a. The concentration of Mg^{2+} seemed to have no effect on the association constant, however, in the range 0–5 mM. At higher concentrations, Mg^{2+} inhibited the interaction: at 50 mM, K_a was reduced 20-fold, and by 500 mM, no binding was observed even at 10 μM coat protein. The behavior of Ca^{2+} and Cu^{2+} was essentially identical with that of Mg^{2+}. The finding that Mg^{2+} can be removed from TMK buffer without affecting the interaction is probably due to the relatively high concentrations of Tris and K^+ in the binding buffer.

A number of components had no effect on K_a when added to TMK. These included β-mercaptoethanol at concentrations up to 10 mM, dimethyl sulfoxide up to 5%, sodium dodecyl sulfate up to 1 μM, and 0.8 mM putrescine plus 0.1 mM spermidine. As was seen in Figure 3, replacing the Tris-HCl buffer with Hepes or other sulfonic acid buffers did not significantly alter the K_a.

Ionic Strength Dependence of K_a. Protein excess binding curves were obtained at various KCl concentrations in the presence of 10 mM magnesium acetate and 0.1 M Tris-HCl, pH 8.5, at 2 °C. In Figure 6, $\log K_a$ is plotted vs. the log of the total cation concentration. The affinity constant decreases with increasing ionic strength over the range 0.1–1.0 M, suggesting that ionic contacts contribute to the RNA–protein interaction. Two types of ionic effects can potentially account for the slope of Figure 6, since the concentrations of both cations and anions are increasing. At high ionic strength, any anion binding sites on the protein are occupied to a greater extent. If the sites occupied by anions are the same ones occupied by the RNA, then competition between these two ligands will reduce the K_a. Alternatively, anion binding to a specific site on the protein could alter the conformation of the protein to a form that binds RNA less well. Although the binding of cations to the RNA is, as in the case of DNA (Manning, 1969, 1978), presumably not governed by mass action, the increased cation concentration can also affect the RNA–protein interaction. Cations displaced from the surface of the RNA upon coat protein binding contribute less favorable entropy of dilution as the ionic strength increases and could thus account for the observed reduction in K_a.

Record and co-workers (Record et al., 1976; Lohman et al., 1980) have developed a quantitative analysis of the salt dependence of K_a based on ion displacement. Application of their interpretation to the R17 case requires several untested assumptions and thus leads only to an upper limit of the number of ionic interactions. If we entirely neglect the effect of anions, assign a value of $\psi_{21\text{-mer}} = 0.85$ on the basis of homopolymer data (Record et al., 1976), and approximate the salt dependence of magnesium binding to the 21-mer from the behavior of homopolymers (Record et al., 1976), we obtain an upper limit of five nucleotide phosphates involved in ion pairs with lysine-like cationic groups on the coat protein. The presence of 10 mM magnesium in the binding buffer adequately explains the leveling off of K_a at low ionic strength in Figure 6, since magnesium can compete effectively with the protein for the RNA phosphates at low salt concentrations.

The nonelectrostatic contribution to the stability of the protein–RNA complex can be estimated from the K_a at 1 M salt, where the electrostatic contributions are minimal (Record et al., 1976; Manning, 1969, 1978). Extrapolating the data in Figure 6, we find $\Delta G = -7.6$ kcal/mol at 1 M salt. Lohman et al. (1980) estimate that each lysine–phosphate-type ion pair contributes only about +0.2 kcal/mol at 1 M salt. Using their estimate and our upper limit of five ion pairs of the lysine–phosphate type, we obtained a $\Delta G_{\text{nonelectrostatic}}$ of −8.6 kcal/mol. Comparison of this value with the observed ΔG in TMK buffer reveals that, under the latter more physiological conditions, at least 80% of the total binding free energy is contributed by nonelectrostatic contacts. Thus, the free energy of the coat protein–RNA interaction is dominated by the nonelectrostatic contribution in spite of the formation of up to five ionic contacts.

Discussion

This paper investigates several properties of the interaction of the R17 coat protein with its specific RNA binding site. The types of experiments and the methods of data analysis used here were developed to evaluate the interaction of the *lac* repressor with DNA fragments containing the *lac* operator (Record et al., 1977; Strauss et al., 1980; Barkley et al., 1981; Berg et al., 1981). Both these systems are examples of regulatory proteins which operate by binding specifically to a relatively small site on a large polynucleotide. Even though in this work we studied the isolated polynucleotide binding site, whereas the *lac* operator in generally studied in the presence of attached nonspecific DNA, it is still appropriate to compare the two protein–nucleic acid interactions. R17 coat protein binds to the isolated fragment with about the same affinity as to intact R17 RNA and shows very little affinity for other RNA sequences (Carey et al., 1983). The contribution of nonoperator sequences to the *lac* repressor–DNA interaction can be minimized by a judicious choice of solution conditions. Thus, the properties of these two sequence-specific protein–nucleic acid interactions can be compared directly. Any differences seen between the two might reflect the large differences in structure between double-stranded DNA and single-stranded RNA.

The association and dissociation rates of the R17 coat protein–21-mer interaction are relatively rapid. At 2 °C in TMK buffer, the half-life of the complex is approximately 1 min. This rapid dissociation rate prohibited use of an excess of nonradioactive RNA to quench association reactions and thus precluded more precise determination of the forward rate

constant. However, the value obtained from the forward rate is somewhat slower than that expected (Alberty & Hammes, 1958) for a diffusion-controlled reaction between molecules the size of the 21-mer and the coat protein monomer. Furthermore, the ratio of the rate constants does not agree precisely with the association constant determined directly from the filter assay. Thus, it remains possible that instead of a simple bimolecular equilibrium, one or more first-order intermediate steps occur in the association pathway.

It is likely that the mechanism for the interaction of coat protein with intact R17 RNA is very similar to the coat protein–21-mer interaction. Since the affinity constants of the two RNAs for the protein are similar (Carey et al., 1983), the rate constants of these interactions are likely to be similar as well. Furthermore, Berzin et al. (1978) found that the association rate of the 59-nucleotide protected fragment is very similar to that of the intact R17 RNA. Thus, the more complicated "bind-and-slide" mechanism of the *lac* repressor that is responsible for very different kinetics (Winter et al., 1981) is not observed with the RNA binding protein. A simple collisional mechanism is further supported by the absence of a measurable association of R17 coat protein with other RNA sequences (Carey et al., 1983). Since other RNAs are unlikely to contain sites with the same complex three-dimensional structure required for binding, collisions between the coat protein and these RNAs are not productive. R17 coat protein, therefore, "finds" the correct site on R17 RNA as a result of a correct collision event.

The values of the thermodynamic parameters describing the R17 coat protein–RNA interaction are also different from those of the *lac* repressor–operator interaction. For the R17 system at 24 °C in TMK buffer, $\Delta G = -9.8$ kcal/mol, $\Delta H = -19$ kcal/mol, and $\Delta S = -30$ cal mol^{-1} deg^{-1}. For the *lac* repressor–operator interaction at 24 °C in 0.2 M NaCl–3 mM Mg^{2+} buffer, de Haseth et al. (1977) find $\Delta G = -16$ kcal/mol, $\Delta H = +8.5$ kcal/mol, and $\Delta S = +81$ cal mol^{-1} deg^{-1}. The nearly 2-fold difference in ΔG probably reflects the very different intracellular concentrations of protein and nucleic acid target sequence under which the two systems must operate. There is, however, a striking contrast in the source of contributions to ΔG for the two systems. The R17 interaction has a large, favorable ΔH which is partially offset by an unfavorable ΔS. In contrast, the *lac* interaction has an unfavorable ΔH and a very favorable ΔS. Favorable ΔH generally results from the establishment of relatively weak contacts of the van der Waals' and hydrogen-bond types, while ionic bonds and hydrophobic forces contribute favorably to ΔS (Beaudette & Langerman, 1980). Thus, the R17 system is apparently characterized by a large number of sites of weak contact between the protein and the RNA. The negative entropy suggests that complex formation may be accompanied by unfavorable hydrophobic interactions or configurational constraints that are not entirely compensated by the ionic component of the interaction.

The effect of monovalent ions on the R17 coat protein–RNA interaction is qualitatively quite similar to that of the *lac* system. Different monovalent cations show no effect on K_d, while anions have a substantial effect, with K_d for the R17 interaction decreasing about 50-fold along the lyotropic series. These data are explained in terms of the different roles that cations and anions play in the interaction. The cations tested bind equally well to nucleotide phosphates, but anions bind differentially to the protein.

An estimate of the number of ionic contacts between nucleotide phosphates and protein basic amino groups can be made from the dependence of K_d on ionic strength. The value we obtain depends on the validity of our assumptions that Mg^{2+} is equivalent to monovalent cations in competing in the ionic interaction and that the influence of anions is not quantitatively significant. An upper limit of five ionic contacts are made between the protein and the RNA.

The study of several DNA binding proteins, notably the *lac* repressor, has led to the notion that ionic contacts are the hallmark of nonspecific protein–nucleic acid interactions. Since in the R17 case both kinetic evidence and competition analysis indicated the absence of nonspecific RNA binding by the coat protein, it was of interest to attempt to reconcile the possibility of as many as five ionic contacts with the apparent lack of a nonspecific binding mode. While ionic contacts are not generally thought to confer specificity on DNA–protein interactions, they may well contribute to specificity in RNA–protein binding. Protein binding sites on RNA molecules are characterized by secondary and tertiary RNA structures which result in unique three-dimensional arrays of nucleotide phosphates. Thus, unlike DNA, in which all phosphates are in an identical pattern and therefore inherently unable to contribute to specificity, an RNA molecule presents to a binding protein a highly textured electrostatic surface. Hence, the structure of RNA enables ionic contacts to contribute to specificity in the protein–nucleic acid interaction.

The results presented here permit us to estimate the K_d for the R17 coat protein–RNA interaction in the infected cell. Assuming an intracellular pH of 7.0 and an effective salt concentration of 0.2 M (von Hippel, 1979), we calculate that at 37 °C the dissociation constant for the interaction is about 3 μM. This value is in excellent agreement with the intracellular concentration of coat protein, which we calculate from the data of Nathans et al. (1969) to be 5–10 μM at the time of repression. Thus, the value of K_d determined from the filter assay by using the synthetic 21-mer appears to be physiologically reasonable.

Registry No. 21-mer, 82642-77-1.

References

Alberty, R. A., & Hammes, G. G. (1958) *J. Phys. Chem. 62*, 154.

Barkley, M. D., Lewis, P. A., & Sullivan, G. E. (1981) *Biochemistry 20*, 3842–3851.

Beaudette, N. V., & Langerman, N. (1980) in *CRC Critical Reviews in Biochemistry*, pp 145–169, CRC Press, Cleveland, OH.

Berg, O. G., Winter, R. B., & von Hippel, P. H. (1981) *Biochemistry 20*, 6929–6948.

Berzin, V., Borisova, G. P., Cielens, I., Gribanov, V. A., Jansone, I., Rosenthal, G., & Gren, E. J. (1978) *J. Mol. Biol. 119*, 101–131.

Carey, J., Cameron, V., de Haseth, P. L., & Uhlenbeck, O. C. (1983) *Biochemistry* (preceding paper in this issue).

de Haseth, P. L., Lohman, T. M., & Record, M. T., Jr. (1977) *Biochemistry 16*, 4783–4790.

Gralla, J., Steitz, J. A., & Crothers, D. M. (1974) *Nature (London) 248*, 204–208.

Krug, M., de Haseth, P. L., & Uhlenbeck, O. C. (1982) *Biochemistry 21*, 4713–4720.

Lohman, T. M., de Haseth, P. L., & Record, M. T., Jr. (1980) *Biochemistry 19*, 3522–3530.

Manning, G. (1969) *J. Chem. Phys. 51*, 924–933.

Manning, G. (1978) *Q. Rev. Biophys. 11*, 179–246.

Nathans, D., Oeschger, M. P., Polmar, S. K., & Eggen, K.

(1969) *J. Mol. Biol. 39*, 279–292.
Record, M. T., Jr., Lohman, T. M., & de Haseth, P. L. (1976) *J. Mol. Biol. 107*, 145–158.
Record, M. T., Jr., de Haseth, P. L., & Lohman, T. M. (1977) *Biochemistry 16*, 4791–4795.
Riggs, A. D., Bourgeois, S., & Cohn, M. (1970) *J. Mol. Biol. 53*, 401–417.
Strauss, H. S., Burgess, R. R., & Record, M. T., Jr. (1980) *Biochemistry 19*, 3504–3515.
von Hippel, P. H. (1979) in *Biological Regulation and Development* (Goldberger, R. F., Ed.) pp 279–347, Plenum Press, New York.
von Hippel, P. H., & Schleich, T. (1969) in *Structure and Stability of Biological Macromolecules* (Timasheff, S., & Fasman, G., Eds.) pp 417–574, Marcel Dekker, New York.
Weber, K. (1967) *Biochemistry 6*, 3144–3154.
Winter, R. B., Berg, O. G., & von Hippel, P. H. (1981) *Biochemistry 20*, 6960–6970.

Nuclear Overhauser Experiments at 500 MHz on the Downfield Proton Spectrum of a Ribonuclease-Resistant Fragment of 5S Ribonucleic Acid†

M. J. Kime and P. B. Moore*

ABSTRACT: The downfield (9–15 ppm) proton NMR spectrum of a RNase A resistant fragment of *E. coli* 5S RNA has been studied by nuclear Overhauser methods. The fragment comprises bases 1–11 and 69–120 of the parent molecule [Douthwaite, S., Garrett, R. A., Wagner, R., & Feunteun, J. (1979) *Nucleic Acids Res. 6*, 2453–2470]. The nuclear Overhauser data identify two double helical structures in the fragment whose sequences are $(GC)_3(AU)(GC)_3$ and $(GC)_2(AU)(GU)$. These structures correspond exactly to the central portions of the terminal stem and procaryotic loop helices which should exist in the fragment sequences according to the Fox–Woese model [Fox, G. E., & Woese, C. R. (1975) *Nature (London) 256*, 505–506] of 5S RNA secondary structure. The significance of these and other nuclear Overhauser effects detected for the structure of 5S RNA and its fragment is discussed.

5S ribonucleic acid and its complexes with ribosomal protein constitute a convenient, low molecular weight system in which the general problem of the interactions of proteins with RNA may be examined. Since the discovery of this molecule in the early 1960s (Rosset & Monier, 1963) a wide variety of genetic, chemical, and physical experiments have been done in an effort to elucidate its structure and the nature of its interactions with proteins [for review see Monier (1974), Zimmermann (1980), and Garrett et al. (1981)]. Among the physical methods brought to bear on this problem has been nuclear magnetic resonance (NMR).

Around 1970 it was demonstrated that nucleic acids dissolved in H_2O give proton resonances between 10 and 15 ppm due to hydrogen-bonded imino protons in base pairs (Kearns et al., 1971a,b). Since relative to the total number of protons in a nucleic acid molecule so few protons contribute resonances in this region, and since the protons which resonate in this region are directly involved in the interactions which stabilize nucleic acid structure, it was clear that interpretation of the downfield region of a nucleic acid proton NMR spectrum was likely to be both feasible and revealing. Work on this kind of spectroscopy has been vigorously pursued ever since [for reviews see Kearns & Shulman (1974), Kearns (1976, 1977), Reid & Hurd (1977), Schimmel & Redfield (1980), and Reid (1981)].

While tRNAs have been the natural nucleic acids which have received the most attention from NMR spectroscopists, 5S RNA, the next largest, abundant RNA, has also been examined. The goal of most proton NMR studies on 5S RNA has been to determine the number of hydrogen bonds in that molecule under different conditions (Wong et al., 1972; Kearns & Wong, 1974; Burns et al., 1980; Luoma et al., 1980; Salemink et al., 1981). In many cases ring current shift calculations have been done to test models of 5S structure against observed downfield proton spectra. Specific resonances in the downfield spectrum of 5S, however, have not been assigned. The downfield spectra given by 5S RNA samples are substantially less well resolved than those of most tRNAs. Given the difficulties which have beset the assigning of tRNA imino resonances until very recently [see Reid (1981), Roy & Redfield (1981), Sanchez et al. (1980), and Schimmel & Redfield (1980)], it hardly seemed worthwhile to pursue assignments in 5S RNA. Without detailed assignments, of course, much of the information which could be gained from studies of the 5S downfield spectrum is lost.

Three years ago it was shown that a large fragment of 5S RNA from *E. coli* can be obtained from it by limited nuclease digestion. The fragment is about half the molecule, consisting of bases 1–11 and 69–120 (Douthwaite et al., 1979), usually with some breakage at bases 87, 88, or 89. Recently it was shown that this fragment has a structure remarkably similar to that of the same sequences in the intact molecule (Kime & Moore, 1983). Its downfield NMR spectrum is a subset of the spectrum of the whole molecule; all structures giving rise to observable downfield features in the fragment spectrum must also exist in the parent molecule. Because the fragment spectrum has fewer resonances and its line widths are narrower, it is far easier to work with than that of the parent molecule. The study of the 5S fragment spectrum offers a means for understanding the structure of the parent molecule, just as the study of nucleolytic fragments of tRNA assisted in the understanding of tRNA spectra (Lightfoot et al., 1973; Kearns & Shulman, 1974; Reid et al., 1979).

† From the Department of Chemistry, Yale University, New Haven, Connecticut 06511. *Received December 13, 1982.* This research was supported by a grant from the National Institutes of Health (AI-09167) to P.B.M. M.J.K. is a NATO/SERC postdoctoral fellow.

0006-2960/83/0422-2615$01.50/0